ULTRASTRUCTURE AND CHROMATIN DISAGGREGATION OF HUMAN SPERM HEAD WITH THIOGLYCOLATE TREATMENT

BEN LUNG. From the Department of Histology and Embryology, School of Dentistry, University of Maryland, Baltimore, Maryland 21201

INTRODUCTION

The active interest in determining the ultrastructural organization of ejaculated human sperm nucleus by the normal thin-sectioning technique has led to a state of understanding that is still incomplete. The findings obtained by this method show that the nuclei of intact human sperm heads are either homogeneously opaque and devoid of visible detail or are tessellated and exhibit faint clumpings and granulations of chromatin material (1, 3, 6, 20, 25, 27).

Whole-mount electron microscopy of bull and human sperm heads has shown that the nucleus can be exposed and that the surrounding membranes can be removed by treatment with alkaline thioglycolate to reduce the disulfide bonds. By this treatment the nucleus was observed to contain chromatin that is strikingly fibrillar (18).

This investigation reports the observations made on ejaculated human sperm nuclei previously treated with alkaline thioglycolate and compared by thin-section and whole-mount electron microscopy.

MATERIALS AND METHODS

Fresh human semen was processed no later than 12 hr and in some cases less than a few hours after emission. The samples were diluted with Tyrode's solution to a volume of 10 ml and washed three successive times by 15-min centrifugations at 500 g.

The washed sperm samples were then treated with alkaline thioglycolate (18). A 0.8 M concentration of alkaline thioglycolate was prepared by raising the pH to 9 with 1 N NaOH. This reagent was mixed 1:1 or 1:2 with the sperm solution. The reaction period ranged from 1 to 5 min and was followed by phase-contrast microscopy. The reaction was stopped by dilution of the thioglycolate with Tyrode's solution. The treated spermatozoa were then immediately centrifuged three times at 500 g for 15 min each in Tyrode's solution.

After the last washing the sperm pellets were fixed in 2.5% glutaraldehyde buffered with phosphate at pH 7.2 (23). The pellets were postfixed with Palade's 2% osmium tetroxide at pH 7.2 (19). Dehydration was carried out with ethanol. The pellets were embedded in Epon 812 and thin-sectioned with the Porter-Blum MT 2B Ultramicrotome. Sections were stained with either uranyl acetate or Reynold's lead citrate (21) and examined with the Siemens Elmiskop I.

Some sperm samples were also processed for whole-mount electron microscopy by employing the Anderson critical point drying method (2). After washing, the treated samples were dehydrated through ascending concentrations of ethanol and transferred to amyl acetate. The samples were then dried in liquid carbon dioxide raised above its critical point temperature in the Anderson critical point apparatus.
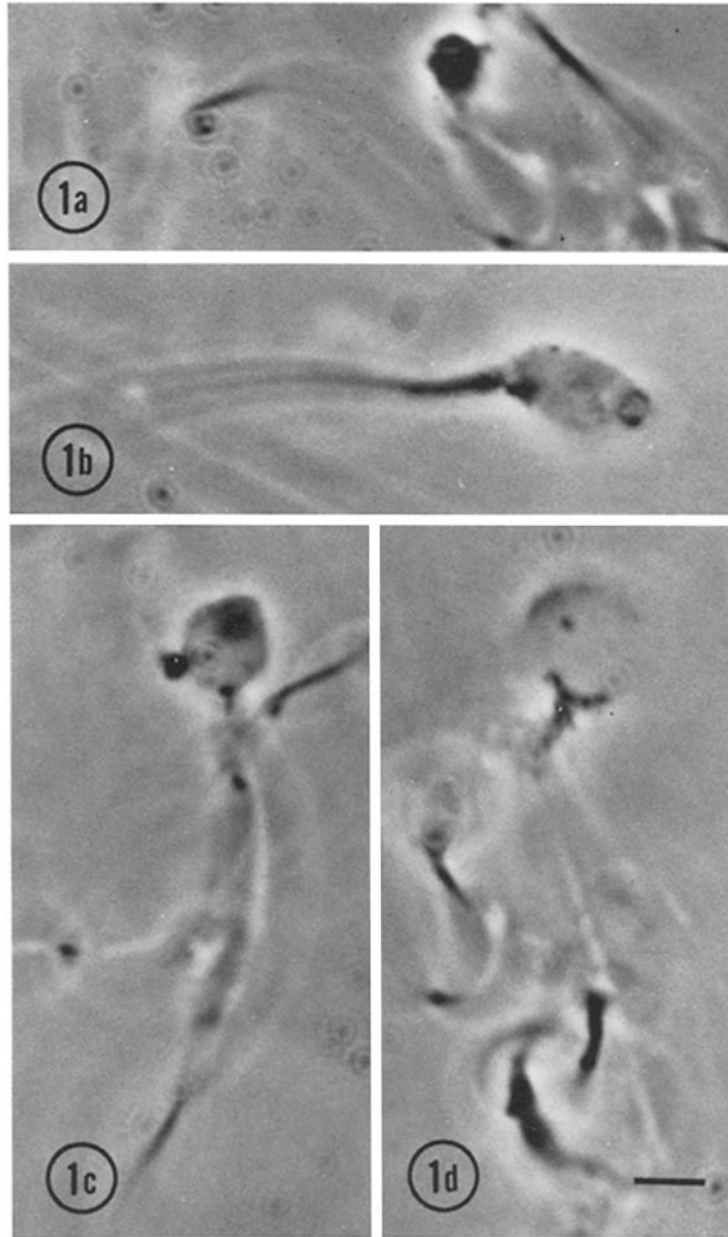
Relative quantitative measurements of human

FIGURE 1   Human sperm treated with alkaline thiogycolate and followed by phase-contrast microscopy. Fig. 1 a shows an early stage of treatment. The sperm head membranes are relatively intact. Fig. 1 b, the head membranes have ruptured and the exposed nucleus begins to expand. A portion of the acrosomal cap is attached to the nucleus tip. Fig. 1 c, the nucleus becomes diffuse with the acrosomal cap still adhering to the tip. Fig. 1 d, the final stage of nuclear exposure showing the head cap expelled and the nucleus in an expanded state. Scale marker, 5 μ. $\times$ 1900.

sperm fiber cross-sections were carried out on the electron micrographs with a high-resolution scannign densitometer (VEB Zeiss, Jena, East Germany) coupled to a stripchart recorder. Areas under the stripchart curves were measured with a Keuffel & Esser Ott–planimeter. These instruments were kindly provided by Dr. G. F. Bahr, Armed Forces Institute of Pathology, Washington, D.C.

RESULTS

Phase-Contrast Microscopy

Treatment with alkaline thioglycolate allows the human sperm head to be freed of its membrane enclosures. The result is a progressive unpacking of the nuclear chromatin. Fig. 1 is a series of phase-contrast micrographs following the rupturing of the head membranes and the exposing of the nucleus after thioglycolate treatment. Initially, the sperm head is reasonably intact (Fig. 1 a). As the reaction proceeds, the acrosomal cap remains attached to the anterior tip (Figs. 1 b and 1 c). Finally, the nucleus becomes more diffuse, and the acrosomal cap is shed, leaving the unpacked nucleus (Fig. 1 d). In many cases, the acrosomal cap in this last stage is not detached but remains seated at the tip of the expanded nucleus.

Electron Microscopy

The thin-sectioned spermatozoa observed in the electron microscope compare favorably with those observed in the light microscope. Observed by phase-contrast microscopy, individual spermatozoa were reactive asynchronously to thioglycolate. Possibly, this was due to different contact times during mixing. Treatment of the sperm solution with 1:1 thioglycolate resulted in most of the sperm reaching the expanded stage after 5 min. In the electron microscope study, the most precise method was to correlate the state of nuclear unpacking with that observed in the phase-contrast study. The sperm head was partially intact in the early stages (Figs. 2–4), comparing approximately to Fig. 1 a. The later stage of Fig. 5 compares to Figs. 1 b and 1 c. Fig. 6 compares to Fig. 1 d.

Upon treatment with thioglycolate, the acrosomal cap containing the acrosome may either immediately detach from the nucleus (Fig. 2) or remain closely adherent to it (Figs. 3 and 4). As seen by thin-section microscopy, the nucleus in the initial stage is still comparatively condensed, showing internal disaggregation of chromatin into clumps and apparent granules (Fig. 2). The granules in this and later stages (Figs. 3–6) are in reality the chromatin fibers as seen by whole-mount microscopy (Figs. 7 a and 8 a) and represent the cut ends of fibers. The fibers in the initial stage have diameters ranging from 450 to 600 A. As the reaction continues, the chromatin fibers begin to disperse (Figs. 3 and 4) and the nucleus becomes progressively diffuse until the whole structure is quite expanded (Fig. 5). Nuclear vacuoles present in the earlier stages are no longer visible in the expanded stage (Fig. 5). Distinct chromatin fibers can now be seen with diameters ranging from 225 to 380 A. Connections of fibers sectioned longitudinally that have smaller diameters of 170–240 A may also be seen. In the final stage, the nucleus becomes even more expanded (Fig. 6). The rupturing and detachment of the membranes is complete, and only remnants are still attached. The chromatin fibers are no longer clumped but uniformly distributed.

As reported in a previous study, the thioglycolate-treated human sperm nucleus seen by whole-mount electron microscopy is fibrillar (18). In many cases, the fibers were found interconnected by cross-fibers or branching points that could represent parallel strands that have separated from their thicker trunks. High resolution microdensitometric scans were made on the cross-sections of such fibers at their branching arms and trunks (Figs. 7 a and 8 a). The strip-chart recordings show that the relative dry mass areas beneath the curves of branching arms, similar in diameter, have sums approximating the dry mass of their trunk (Figs. 7 a and 7 b). Some of the arms having unequal fiber diameters and accordingly unequal masses also had sums approximating the dry mass of their trunk (Figs. 8 a and 8 b). The trunks revealed no visible detail of intrafiber disjunction, except in a rare instance where a less electron-opaque area was observed paralleling the median of the trunk.

DISCUSSION

Unlike that of most mammalian sperm, the nucleus of the ejaculated intact human sperm does not reach the same degree of homogeneity and opacity in all cases. Earlier thin-sectioning studies report that the nucleus may be quite homogeneous or coarsely granulated, i.e. comparable to a late spermatid-like nucleus. The presence of granule-like elements seen in the nucleus of ejaculated human sperm is suggestive of incomplete chromatin condensation (3, 20, 27). This suggestion is supported by the fact that both homogeneous and granulated nuclei appear in the same section, and this finding is not considered to be an artifact of preparation (3, 20). Thin-sectioning of ejacu-
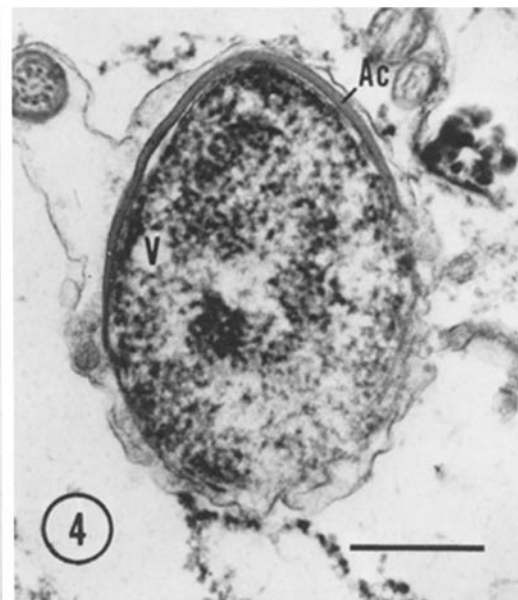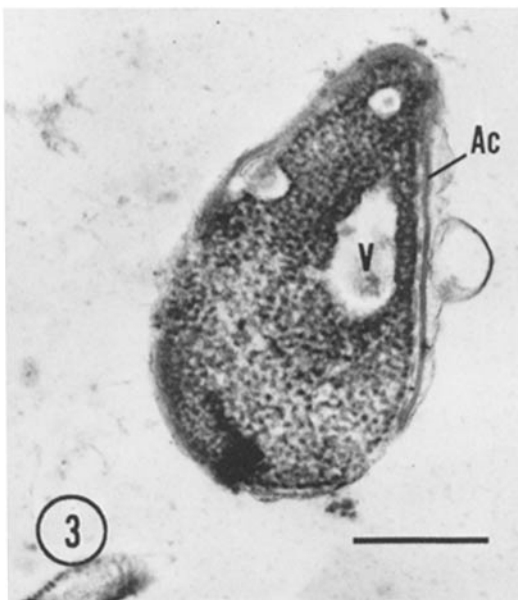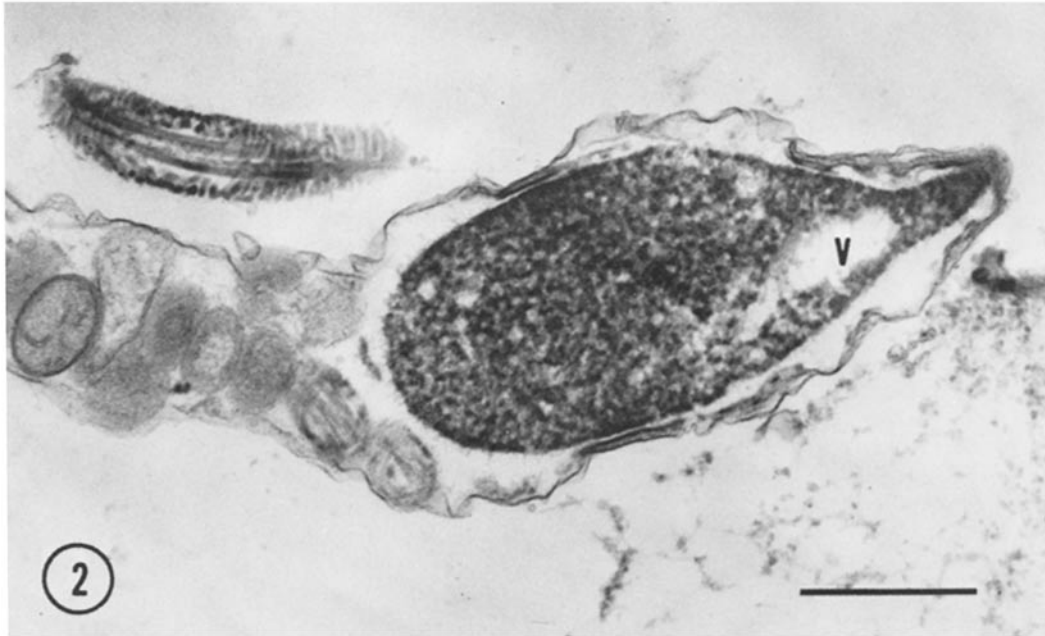
FIGURE 2 Sagittal section through human sperm head at early stage of thioglycolate treatment. The nucleus contains thick and clumped fibrous chromatin, interrupted by anterior vacuole (V). Head membranes in this case are detached early from the nucleus. Scale marker in Figs. 2–6, 1 μ. × 22,300.

FIGURE 3 Human sperm head in sagittal section in a slightly later stage of thioglycolate treatment. Chromatin fibers are in a beginning stage of dispersal. Nuclear vacuoles (V) are present in the anterior portion of the nucleus. The acrosome (Ac) is still attached with a ruptured outer cytoplasmic membrane. × 17,900.

FIGURE 4 Human sperm head in frontal section showing further dispersion of chromatin. Nuclear vacuole (V) is faintly visible. The acrosome (Ac) is attached to the nucleus with the ruptured outer cytoplasmic membrane greatly distended. × 18,100.
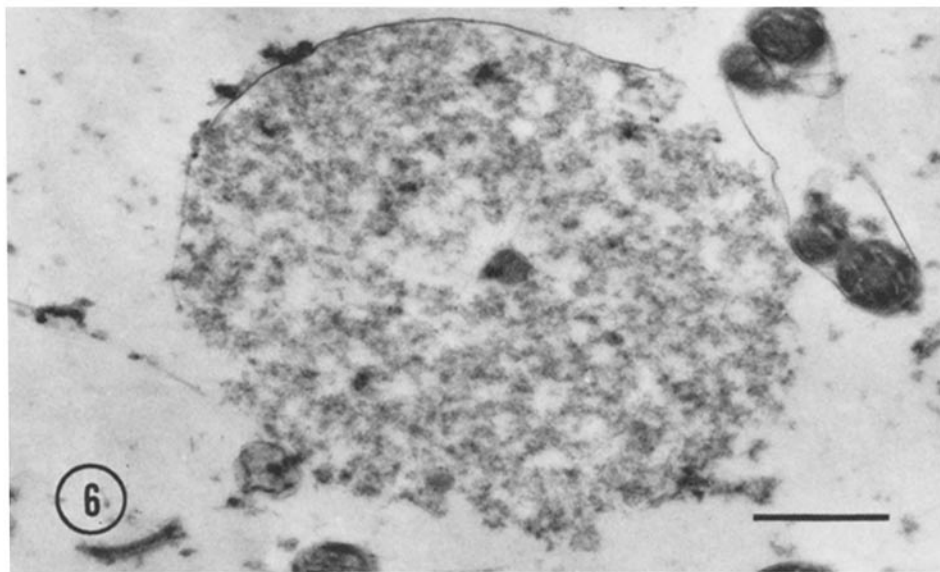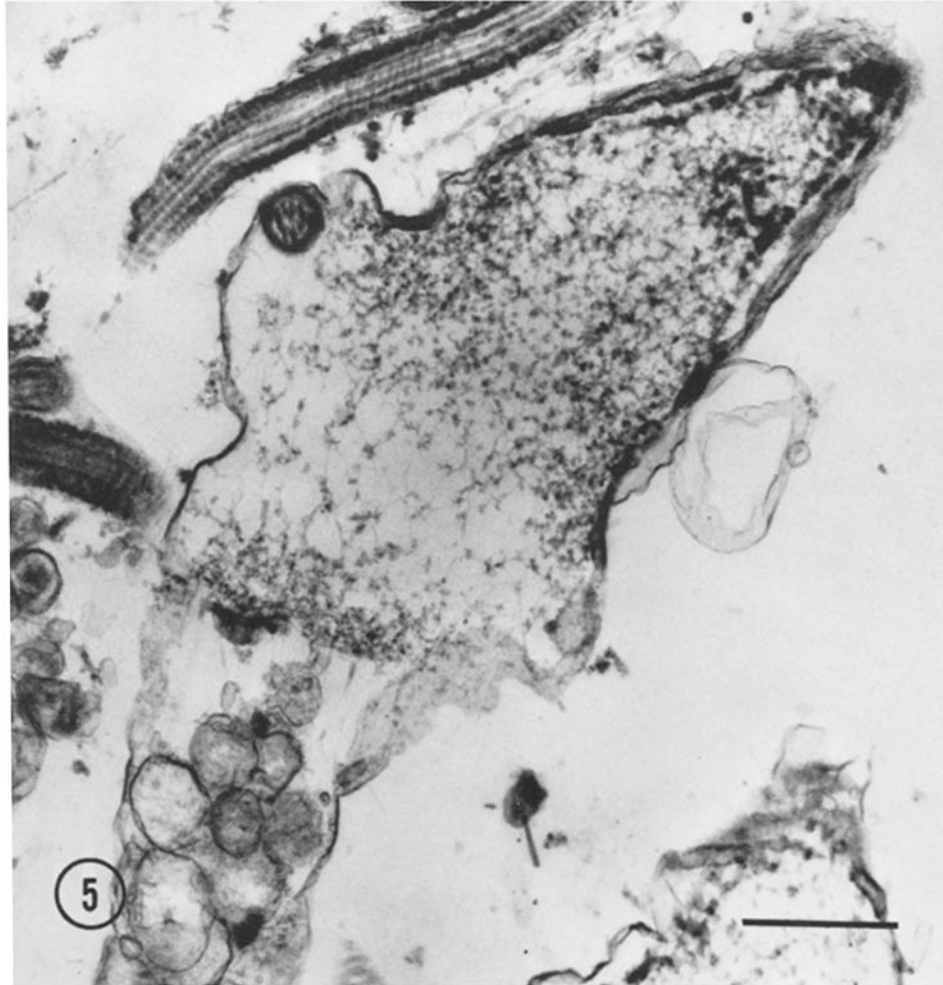
FIGURE 5 Sagittal section of human sperm head with nucleus in expanded stage. The thin chromatin fibers are highly dispersed and undergoing a process of disaggregation. Connections of thin fibers sectioned longitudinally may be seen. The acrosome and head membranes are in a state of disruption (cross-section of sperm tail in superior part of the nucleus belongs to a neighboring sperm). × 20,300.

FIGURE 6 Final stage of nuclear exposure seen in cross-section. Thin chromatin fibers uniformly dispersed with only a nuclear membrane remnant still attached. × 18,000.

lated sperm in the initial stage of alkaline thio-glycolate treatment reveals that the nuclei possess apparent granulations comparable to those of the late spermatid-like nucleus (Fig. 2). The apparent granules in this and later stages do not represent true granules but are the cut ends of fibers produced during sectioning. This observation is confirmed by the chromatin fibers seen with thin-section and whole-mount electron microscopy. Thin-sectioning of the treated sperm
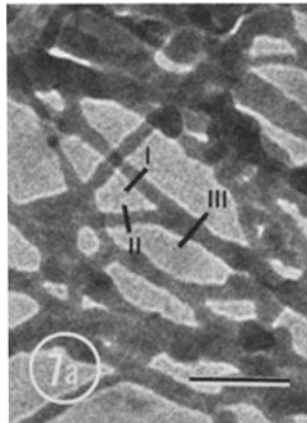

Figure 7 a High magnification of human sperm chromatin fibers showing branching point. High resolution densitometric scans were made of fiber cross-sections at branching points with arms of nearly equal diameters (lines I and II) and trunk (line III). Scale marker in Figs. 7 a and 8 a, 0.1 μ. × 128,200.

reveals the chromatin to lack spatial organization and to contain nuclear vacuoles which may also be seen in the intact sperm.

The alkaline thioglycolate reaction permits one to follow the human sperm chromatin through the process of decondensation and disaggregation (Figs. 2–6). Other sulfhydryl-containing reducing agents were also effective (Lung, unpublished observations). Thick fibers in the early stages of treatment are coarser and more clumped than the fibers appearing in the later stages. The fibers in the late stages are smaller in diameter and more dispersed.

Whole-mount electron microscopy coupled with the microdensitometric scans of fiber branching arms and trunks reveals that the mass sum of the arms approximates the mass of their trunk. This result strongly supports the hypothesis that the trunks are aggregates of the arms. The arm diameters were found to be in agreement with the diameters of the thin-sectioned chromatin fibers observed in the late stages of thioglycolate treatment. This suggests that the arms are undergoing a process of disaggregation.

The disruption of disulfide bonds as a requirement is significant for the in vitro decondensation and disaggregation of mammalian sperm chromatin fibers. The precise location of the disulfide linkages is not known. The formation of disulfide linkages in mammalian sperm occurs during maturation and aids in stabilizing the nuclear chromatin (5). Sadgopal and Bonner (24) re-
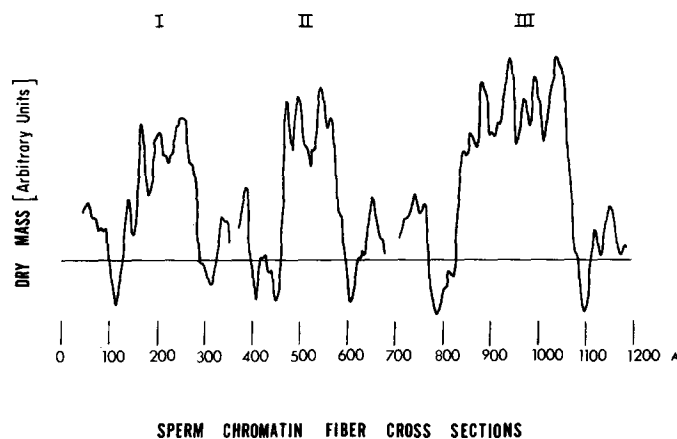

SPERM CHROMATIN FIBER CROSS SECTIONS

Figure 7 b High resolution densitometric tracings of human sperm chromatin fiber cross-section seen in Fig. 7 a. Areas beneath the curves give cross-sectional dry mass of the fiber equivalents in arbitrary units. The dry mass of arm I (curve I, 478 units) and arm II (curve II, 512 units) have sums approximating the mass of the trunk (curve III, 1146 units).

port that the formation of disulfide linkages between chromosomal proteins is important for the interphase-metaphase condensation. Evidence exists that the high sulfur content found in bull sperm resides in the arginine-rich proteins and forms disulfide cross-links within the nucleus (4, 7, 16). A suggestion has been made that the mammalian sperm nuclear protein is rich in sulfhydryl groups which cross link the chromosomes by forming disulfide bonds (10). This interesting

FIGURE 8 a High magnification of human sperm chromatin fibers showing branching point. High resolution densitometric scans were made of fiber cross-section at the branching points of arms with unequal diameters (lines I and II) and trunk (line III). × 128,200.

possibility, however, requires further investigation.

The concept that human sperm chromatin granules are fibers is theoretically in agreement with the finding of fibrillar interphase chromatin by Ris (22), Gall (13), and DuPraw (9), when one compares the granules observed in thin-sectioned interphase nuclei. With the use of either whole-mount or thin-section microscopy, observations of chromatin fibrils in sperm nuclei of various animals have been reported (14, 22, 26, 28, 29). Ris (22) reports that in nonmammalian sperm the condensed sperm nucleus arises from both condensation and aggregation of chromatin fibrils.

The problem of chromatin aggregation has been investigated in human spermiogenesis. Various authors, on the basis of studies of thin sections, interpret the chromatin of human spermiogenic cells to be granular (8, 12, 15, 17). In the early spermatid stage, fine chromatin granules were observed uniformly throughout the nucleus. In the later stages of maturation, the spermatid chromatin granules were found to be coarse and to have larger diameters (8, 12, 17). Horstmann (17) measured the diameters of early spermatid granules and found them to range from 180 to 200 A. The diameters of the granules of the late spermatid stage ranged from 600 to 700 A. Fawcett (11) proposed, on the basis of his earlier study (12), that the dense chromatin arises from aggregation of fine granules. The re-
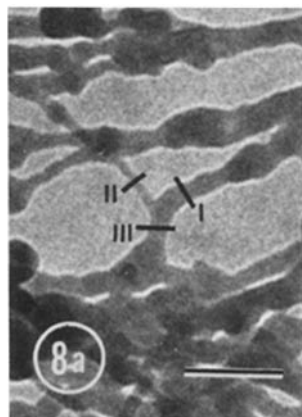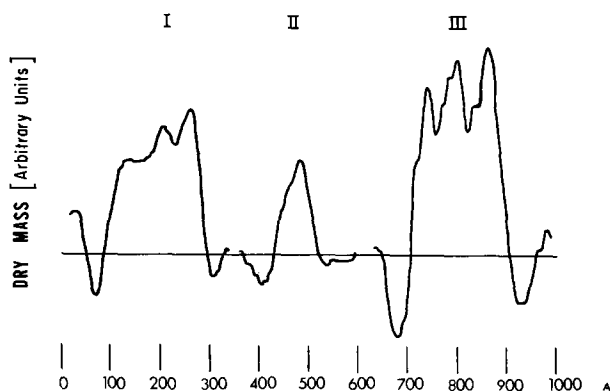

SPERM CHROMATIN FIBER CROSS SECTIONS

FIGURE 8 b High resolution densitometric tracings of human sperm chromatin fiber cross section seen in Fig. 8 a. Areas beneath the curves give cross sectional dry mass of arm I (curve I, 670 units) and arm II (curve II, 157 units) having sums approximating the trunk mass (curve III, 825 units).

sults reported here, based on the observations of chromatin fiber disaggregation by thioglycolate, support Fawcett's proposal of fibrillar rather than granular aggregation.

REFERENCES

1. ANBERG, A. 1957. *Acta Obstet. Gynecol. Scand. Suppl.* 2. **36**:1.
2. ANDERSON, T. F. 1951. *Trans. N. Y. Acad. Sci.* (II) **13**:130.
3. BEDFORD, J. M. 1967. *Amer. J. Anat.* **121**:443.
4. BRIL-PETERSEN, E., and H. G. K. WESTENBRINK. 1963. *Biochim. Biophys. Acta.* **76**:152.
5. CALVIN, H. I., and J. M. BEDFORD. 1971. *J. Reprod. Fert.* (Suppl.) **13**:65.
6. CHRZANOWSKI, S. 1966. *Pol. Med. J.* **5**:482.
7. COELINGH, J. P., T. H. ROZIJN, and C. H. MONFOORT. 1969. *Biochim. Biophys. Acta.* **188**:353.
8. DEKRETSER, D. M. 1969. *Z. Zellforsch. Mikrosk. Anat.* **98**:477.
9. DUPRAW, E. J. 1965. *Proc. Nat. Acad. Sci. U. S. A.* **53**:161.
10. DUPRAW, E. J. 1970. DNA and Chromosomes. Holt, Rinehart & Winston, Inc., New York. 278.
11. FAWCETT, D. W. 1958. *Int. Rev. Cytol.* **7**:195.
12. FAWCETT, D. W., and M. H. BURGOS. 1956. *Ciba Found. Colloq. Ageing* **2**:86.
13. GALL, J. G. 1963. *Science (Washington).* **139**:120.
14. GRIGG, G. W., and A. J. HODGE. 1949. *Aust. J. Sci. Res. Ser. B.* **2**:271.
15. GUILLON, M. G. 1960. *Bull. Fed. Soc. Gynecol. Obstet. Lang. Fr.* **12**:531.
16. HENDRICKS, D. M., and D. T. MAYER. 1965. *Exp. Cell Res.* **40**:412.
17. HORSTMANN, E. 1961. *Z. Zellforsch. Mikrosk. Anat.* **54**:68.
18. LUNG, B. 1968. *J. Ultrastruct. Res.* **22**:485.
19. PALADE, G. E. 1952. *J. Exp. Med.* **95**:285.
20. PEDERSEN, H. 1969. *Z. Zellforsch. Mikrosk. Anat.* **94**:542.
21. REYNOLDS, E. S. 1963. *J. Cell Biol.* **17**:208.
22. RIS, H. 1961. *Can. J. Genet. Cytol.* **3**:95.
23. SABATINI, D. D., K. BENSCH, and R. J. BARRNETT. 1963. *J. Cell Biol.* **17**:19.
24. SADGOPAL, A., and J. BONNER. 1970. *Biochim. Biophys. Acta.* **207**:227.
25. SCHULTZ-LARSEN, J. 1958. *Acta Pathol. Microbiol. Scand. Suppl.* **128**:1.
26. SOLARI, A. J. 1965. *Proc. Nat. Acad. Sci. U. S. A.* **53**:503.
27. ZAMBONI, L., R. ZEMJANIS, and M. STEFANINI. 1971. *Anat. Rec.* **169**:129.
28. ZIRKIN, B. R. 1971. *J. Ultrastruct. Res.* **34**:159.
29. ZIRKIN, B. R. 1971. *J. Ultrastruct. Res.* **36**:237.